CHAPTER–6

GEOCHEMISTRY

6.1 Introduction

The term "geochemistry" is composed of two constituent words: "geo," referring to the Earth, and "chemistry," which pertains to the scientific study of chemical transformations. To understand and quantify the chemical composition and structural properties of rocks, a petrologist needs to look for the chemistry of the rock, termed geochemistry. The earth's crustis predominantly comprised of igneous rocks, primary rocks formed from magmas. The nature of metamorphic rock suites can be broadly characterized by major and trace element chemistry. Most metamorphic rocks consist of silicates, combinations of one or more minerals, and naturally occurring inorganic chemical compounds. This section encapsulates the geochemical features of pelitic granulites, garnet-bearing gneisses, and amphibolites from thestudy area. It presents a theoretical model for the evolutionary history of these rocks. To comprehend the tectonic evolution of rocks in the examined region, it is necessary to performa geochemical analysis of metamorphic rocks. The primary objectives of this study are: to determine whether the metapelites and metabasic are of orthometamorphic or parametamorphic origin, To identify the nature of the source magma or the tectonic environment responsible for magma generation, to investigate the extent of depletion of large-ion lithophile elements (LILE) and the enhancement of K/Rb ratios and to compare the chemical characteristics of different metapelites and metabasics with those of similar suites of parent rock.

6.2 Major oxides Geochemistry

Metamorphic rocks are abundant in various oxides, arranged by increasing atomic numbers. These oxides encompass silicon (SiO_2), aluminium (Al_2O_3), titanium (TiO_2), iron (Fe, including ferric Fe_2O_3 and ferrous FeO), calcium (CaO), magnesium (MgO), manganese (MnO), sodium (Na_2O), potassium (K_2O), and phosphorus (P_2O_5). These oxides play a significant role in rock classification and the construction of variation diagrams. Major elements constitute more than 1 wt % of the Earth's crust, while trace elements make up less than 1wt %. The behavior of major oxides in magmas can be explained through differentiation indices and the trace elements behave similarly as they substitute for major elements. Geochemistry and patterns of geochemical variations a potent tools for identifying the protolith of metamorphic rocks, understanding the nature of melts, deciphering magmatic processes, and determining tectonothermal conditions. Numerous discrimination diagrams are utilized to discern whether the protoliths of metamorphic rocks originated from sedimentary or igneous sources.

6.3 Trace Element Geochemistry

Trace element geochemistry plays a significant role in elucidating a rock's evolution and identifying its depositional environment. Trace element abundances provide insights into processes such as crystal fractionation, partial melting, and source composition during evolution. The concentration of these trace elements (Sr, Rb, Nb, Ba, Zr, Hf, Cs, Pb, Ta) in rocks is less than 0.1%, expressed in parts per million (ppm). They aid in studying elemental distribution in crystal-melt equilibria. Compatible trace elements are those favoured in the mineral phase, while

incompatible elements have a preference for melting. Incompatible elements are categorized as high field strength (HFSE) elements (U, Pb, Nb, Hf, Ta, Y, Sc,) and large-ion lithophile elements (LILE) (Rb, Cs, Ba) based on charge-size ratios or ionic potentials.

6.4 Rare Earth Elements Geochemistry

The behaviour of rare earth elements gradually changes from La to Lu. Rare earth element contents in igneous rocks provide insights into magma sources, crustal contamination, degree of partial melting and crystal fractionation during magma evolution. Rare earth elements (REE) are usually immobile after igneous alteration and low-grade metamorphism. REE patterns help in understanding the petrogenesis of magmatic bodies and tectonic settings. REEs consist of 15 trace elements with atomic numbers from 57 (La) to 71 (Lu), 14 of these elements are naturally occurring. They are divided into light rare earth elements from La to Sm and heavy rare earth elements from Gd to Lu, with middle rare earth elements covering elements from Sm to Ho. In natural conditions, all REEs exist in a 3+ oxidation state, except for Ce4+ (oxidized form) and Eu2+ (reduced form).

6.5 Analytical Techniques

For this study, fourteen representative samples from the Makrohar granulite belts of CGGC were subjected to chemical analysis for major, trace, and REE compositions. Geochemical data for various rock samples are presented in Tables 6.1-6.2. To ensure accuracy, fresh samples were selected and processed using various crushing and pulverization methods. Major element analyses were conducted using X-ray fluorescence (XRF), while trace and REE analyses were performed using

Inductive Coupled Plasma-Mass Spectrometry (ICP- MS).

6.5.1 XRF and ICP-MS Analysis

XRF and ICP-MS were used to analyze major oxides, trace elements and rare earth elements. The analysis was conducted at the Birbal Sahni Institute of Palaeosciences (BSIP), Lucknow, Uttar Pradesh, India. The pressed powder method mixed with boric acid as a binder was employed for sample preparation. Major oxide analyses were carried out using XRF, while rare earth elements were analyzed using ICP-MS. Different calibration standards were used to ensure accuracy.

6.6 Metabasics

6.6.1 Major Oxides

The results of the geochemical analysis of garnetiferous amphibolites (S-9, S-10, S-11 and S- 12) and mafic granulites (M-13, M-14, M-15 and M-16) are presented in Table 6.1. The metabasics exhibit significant variability in major oxide composition, encompassing SiO_2 (48.30–50.92 wt%), Al_2O_3 (11.04–15.52 wt%), MgO (4.14–5.85 wt%), FeO (13.17–17.54 wt%) as well as lesser quantities of TiO_2 (0.51–1.85 wt%), CaO (8.53–11.49 wt%), and Na_2O (2.08–2.66 wt%). The Total Alkali versus Silica (TAS) plot is utilized for the classification of metabasics (Le Maitre et al., 1989), (Fig. 6.1a). Here, metabasics align within the basalt field. The Zr/Ti versus Nb/Y diagram (Winchester & Floyd 1977) is used, revealing that all garnetiferous amphibolites fall in the sub-alkaline basalt field while mafic granulites are found in the basaltic-andesite field. SiO2−FeOt MgO plot (Miyashiro, 1974) used to show tholeitic series for the metabasics and Fe^t + Ti-Al-Mg ternary plot (Jensen, 1976) shows high iron tholeiite basalt field for the metabasics (Fig. 6.1c-d).

6.6.2 Trace and REEs

The normalized multi-elemental spider diagram to the primitive mantle is a valuabletool for understanding trace elements within metabasics, aiding in identifying their source regions.A subduction orogeny hallmark is an enrichment of a large ion lithophile element (LILE Rb, Th, Pb, U, K and Y) and a negative anomaly of high field strength element (HFSE Sr, Ti and Nb is evident in the analyzed metabasics (Fig. 6.2a). The decrease in Ti and Nb concentrations provides validation for an island arc setting. Moreover, Rare Earth Element (REE) patterns, normalized to chondrite values, are utilized to elucidate Rare earth element behaviour within the metabasics and to differentiate source compositions (Fig. 6.2b). Garnetiferous amphibolites show a moderate LREE enrichment compared to HREE (LaN/LuN = 1.66–2.38) and a slight negative Eu anomaly (EuN/EuN* = 0.43–0.67). Conversely, mafic granulites exhibit a higher enrichment of Light Rare Earth Elements relative to Heavy Rare Earth Elements (La_N/Lu_N = 3.85–5.49) alongside a slight negative Eu anomaly (EuN/EuN* = 0.75–0.91). The presence of sub-parallel REE patterns suggests the dominance of compositional variation resulting from crystal fractionation. Multiple tectonic discrimination diagrams have been employed to reveal the protolith characteristics of metabasics (Fig. 6.3).

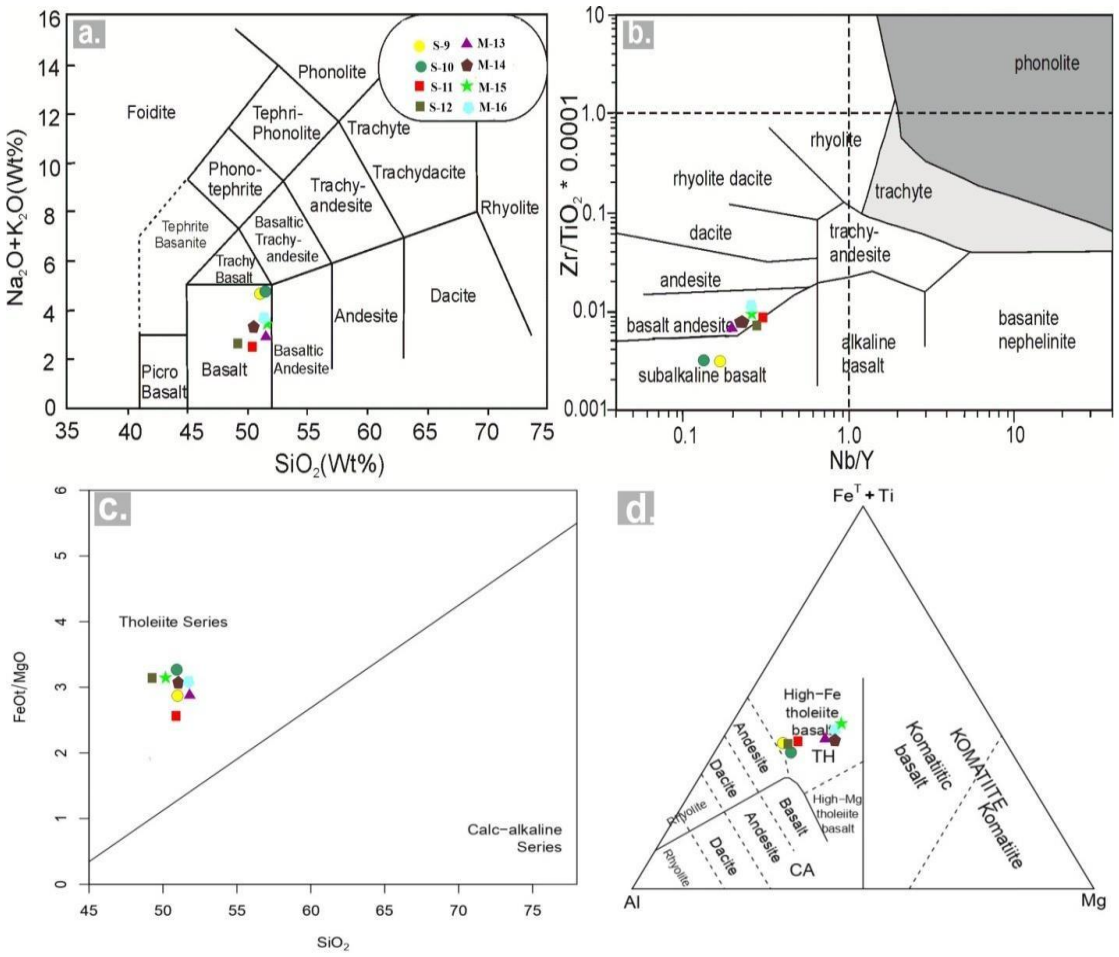

Figure 6.1 (a) Total alkali versus silica (TAS) plot is used to classify metabasics (Le Maitre et al., 1989). (b) The Zr/Ti vs Nb/Y plot (Winchester and Floyd, 1977). (c) SiO2−FeOt MgO plot (Miyashiro, 1974). (d) Fe^t + Ti-Al-Mg ternary plot (Jensen, 1976).

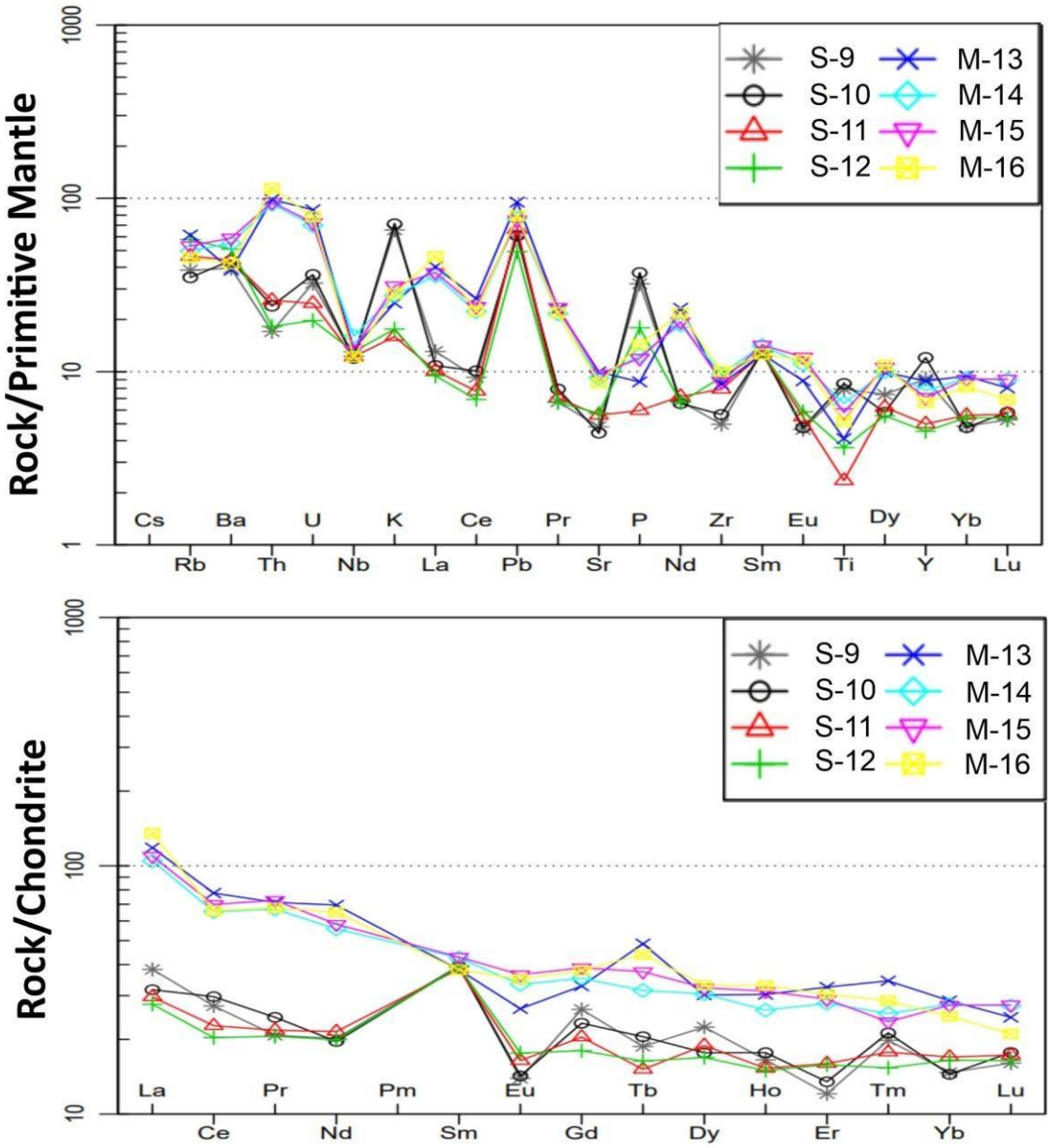

Figure 6.2 (a) Multi-element normalized spider diagram of metabasics(normalized after Sun and McDonough, 1989). (b) Chondrite normalized rare earth element plot (normalized after Anders and Grevesse 1989).

6.6.3 Petrogenesis and tectonic implications

Geochemical data are often utilized to reconstruct the petrogenesis of mantle-derived magmatic rocks. Throughout the Archean, mafic magmatic activity in the form of intrusions or dykes provides a valuable window for observing mantle evolution. More extensive crustal contamination in Archean magma was generated by

higher geothermal and Th/U compositions of juvenile felsic crust (Abbott et al. 1994). This crustal melt inflow may cause isotopic and compositional changes in primary mantle-derived magma or hybrid magma(Martins et al. 2017), as well as subduction-like indications such as negative Ti and Nb anomalies compared to N-MORB, leading to continental intra-plate basalts being falsified as arc basalts (Xia, 2014). The relative diversity of large-ion lithophile elements (LILEs; Rb, Th and U) concentration in subduction zones indicates late-stage modifications caused by the action of subduction-resultant fluids (Guilmette et al., 2009). As a consequence, we propose that metabasics exhibit both spreading and subduction signs, making it difficult todetermine the tectonic setting. After that, it is critical to look for crustal contamination in metabasicsand determine what role it plays in their formation.

6.6.4 Metabasics: Geochemical Insights

The examined amphibolites showed moderate enrichment of Light Rare Earth Elements(LREE) and Large Ion Lithophile Elements (LILEs) such as Rb, K, Y, Pb, Th and U while concurrently displaying negative anomalies in elements like Ti, Zr, Nb, and Sr. Within this context, metabasics present lower Th concentrations ranging from 1.45 to 2.19 ppm. This lowTh content indicates minimal to no contribution from crustal contamination (Pearce etal., 2005). Despite their potential for metamorphism from mafic rocks to high-grade metamorphic states, the petrogenetic characteristics of the meta basics are best measured through immobile trace elements including High Field Strength Elements (HFSEs) such as Nb, Ti, Zr, and Y, Rare Earth Elements (REEs) like Yb, Sm and La transition elements likeV, Y, and Sc, (Mahoney et al., 2000). The tectonic context is closely linked to HFSEs and REEs which are important indicators of the formation of metabasics. The discrimination diagram of Th/Nb vs

Ba/Nb (Pearce & Stern, 2006) signifies the influence of deeper subduction components on mafic granulites (Fig. 6.3a). Furthermore, the Nb/Th vs Zr/Nb discrimination diagram, drawing from Sun & McDonough (1989), indicates an arc-like setting for metabasics (Fig. 6.3b) while the Zr vs Zr/Y plot, following Pearce & Norry (1979), suggests an island arc context (Fig. 6.3c). High Th/Yb and low Nb/Yb ratios corroborate the influence of subduction processes and suggest intra-oceanic arc basalts for garnetiferous amphibolites (Fig. 6.3d) and arc-basalt for mafic granulites. In a tectonic discrimination diagram (Th/Nb vs Ce/Nb) proposed by Saunders et al. (1988), metabasic samples conform to an island basalt setting (Fig. 6.3e). Additionally, in the Y vs La/Nb diagram by Floyd et al. (1991), metabasics align with the Back-Arc Basin Basalts (BABB) field (Fig. 6.3f). These cumulative insights point to the generation of metabasics within a back-arc setting during an extensional regime. It is concluded that the metabasic protolith originated as enclaves of mafic rocks within subduction-related arcs, based on field observations, interrelationship withpelitic rock, geochemical analyses and inferred metamorphic history.

During the Neoarchean era, these rocks collided and went through tectonic activity. Consequently, amphibolite fragments were subjected to peak metamorphic conditions and changed into mafic granulites. They also interacted with fluids derived from the subduction, leading to geochemical changes. Subsequently, the mafic granulites go through retrograde metamorphic changes and transition into amphibolites during the exhumation phase.

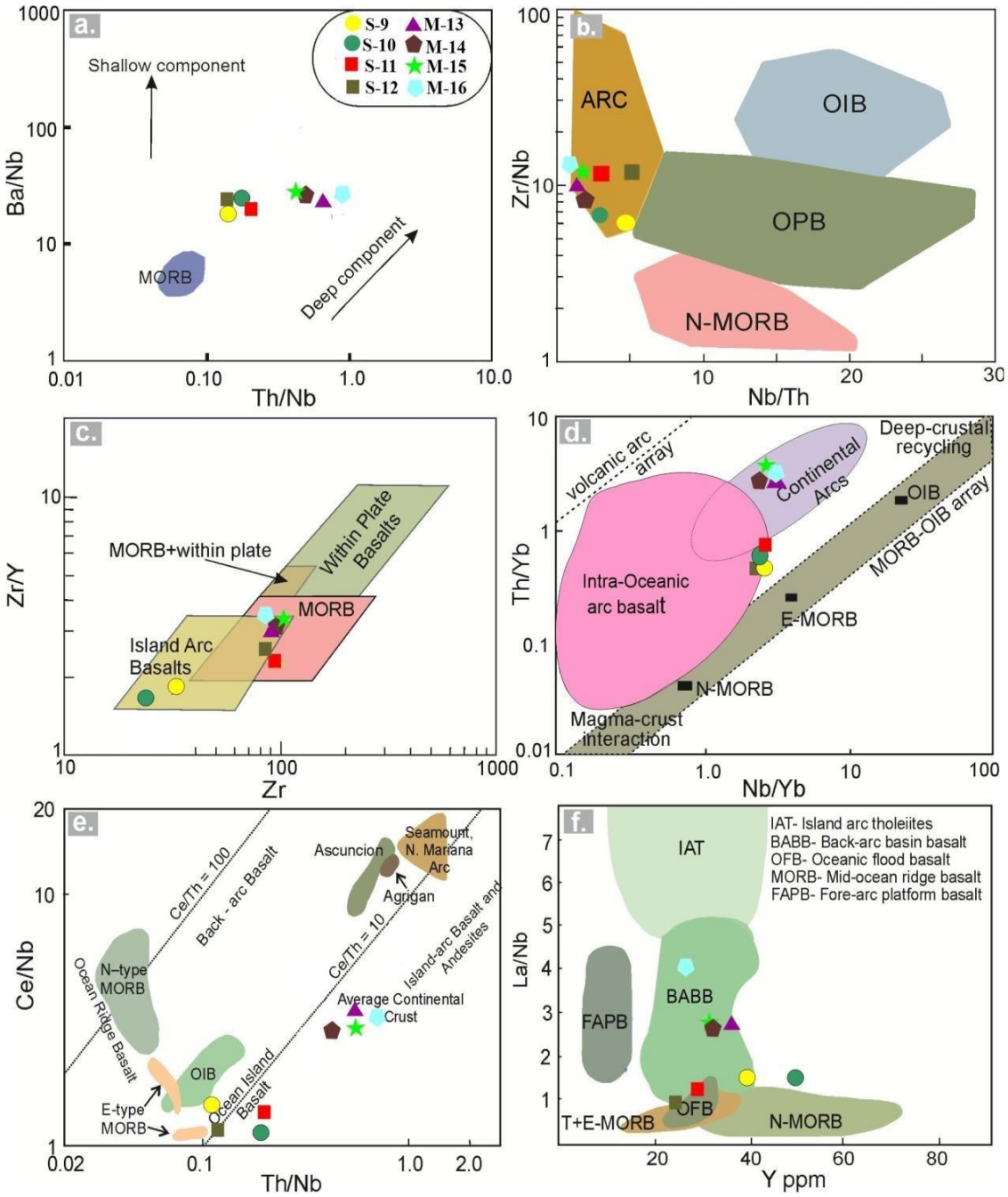

Figure 6.3 (a) Th/Nb vs Ba/Nb diagram (after Pearce and Stern, 2006) showing the influence of deep subductioncomponent in the mantle source for the mafic granulites. (b) Nb/Th vs Zr/Nb diagram indicating the arc nature of the metabasics (after Sun and McDonough, 1989). (c) Zr vs Zr/Y diagram showing the island-arc nature of themetabasics (after Pearce and Norry, 1979). (d) Nb/Yb vs Th/Yb diagram (Pearce, 2008) depicting a subduction-related enrichment for the metabasic samples. Fields for intra-oceanic arc basalt and continental arcs are. (e) Ce/Nb vs Th/Nb plot (after Saunders et al., 1988) showing Island-arc affinity. (f) Y vs La/Nb diagram (modified after Floyd et al., 1991) showing back-arc affinity.

Table 6.1 Representative major oxides (in wt%), trace elements and REEs (in ppm) compositions of metabasic.

Oxides	**S-9**	**S-10**	**S-11**	**S-12**	**M-13**	**M-14**	**M-15**	**M-16**
SiO_2	50.45	50.49	50.03	48.3	50.92	50.23	49.22	50.84
Al_2O_3	14.12	14.25	14.7	15.52	11.42	11.3	11.23	11.04
TiO_2	1.72	1.85	0.51	0.79	0.89	1.42	1.26	1.11
FeO	13.17	13.86	13.89	14.75	17.12	17.54	17.18	16.52
MnO	0.22	0.16	0.21	0.22	0.2	0.22	0.26	0.31
MgO	4.56	4.14	5.34	4.82	5.85	5.41	5.35	5.49
CaO	9.32	8.53	11.49	11.22	9.23	9.31	10.39	9.94
Na_2O	2.36	2.27	2.08	2.1	2.23	2.32	2.66	2.47
K_2O	1.98	2.14	0.48	0.53	0.75	0.83	0.94	0.85
P_2O_5	0.7	0.81	0.13	0.39	0.19	0.27	0.26	0.31
LOI	1.28	1.12	1.07	1.21	0.94	0.87	1.17	0.98
TOTAL	99.88	99.62	99.93	99.85	99.74	99.72	99.92	99.86
Ba	276	306	308	356	269	385	412	293
Cr	367	384	381	408	284	204	304	386
Nb	8.7	8.5	8.7	9.3	9.7	11.4	9.5	8.7
Ni	134	129	125	132	214	196	204	184
Rb	24	22	29	37	39	32	34	29
Sr	101	93	118	121	210	194	203	182
V	285	272	274	266	295	401	384	356
Y	41	55	23	21	40	35	32	30
Zn	105	118	98	90	119	116	113	101
Zr	56	63	88.7	104	95	108	98	112
Sc	36	35	48	45	48	53	55	44
Cu	164	155	162	160	308	323	285	241
Pb	4.4	4.3	4.7	3.5	6.7	5.4	5.3	5.6

Th	1.4	2.0	2.2	1.5	8.3	7.9	8	9.6
Co	52	70	62	59	81	73	75	58
U	0.68	0.76	0.52	0.41	1.8	1.5	1.5	1.6
Ga	22	18	15	16.7	31.4	21.8	23.4	27.4
La	8.9	7.4	6.9	6.5	27.7	24.5	25.6	31.7
Ce	16	18	14	12	47	39	42	39
Pr	1.8	2.2	1.9	1.8	6.3	5.9	6.4	6
Nd	9.1	8.9	9.7	9.0	31.4	25.2	26.3	29.4
Sm	5.8	5.8	5.6	5.7	5.6	6.3	6.3	5.8
Eu	0.78	0.80	0.92	0.99	1.5	1.9	2.0	1.9
Gd	5.2	4.6	4.0	3.5	6.6	6.9	7.6	7.4
Tb	0.68	0.74	0.55	0.59	1.8	1.1	1.4	1.6
Dy	5.4	4.3	4.6	4.1	7.3	7.4	7.8	8.0
Ho	0.92	0.98	0.85	0.83	1.7	1.4	1.7	1.8
Er	1.9	2.1	2.5	2.5	5.2	4.4	4.6	4.8
Tm	0.48	0.51	0.43	0.37	0.83	0.61	0.57	0.69
Yb	2.4	2.3	2.8	2.7	4.6	4.5	4.5	4.0
Lu	0.39	0.43	0.42	0.40	0.60	0.66	0.67	0.51
$(La/Lu)_N$	2.4	1.8	1.7	1.7	4.8	3.8	3.9	5.5
Eu/Eu*	0.43	0.47	0.59	0.67	0.75	0.86	0.89	0.91